Reactivity Switch of Platinum with Gallium: From Reverse Water Gas Shift to Methanol Synthesis

Wei Zhou[1], Enzo Brack[1], Christian Ehinger[1], James Paterson[2], Jamie Southouse[2], Christophe Copéret[1]*

[1]*Department of Chemistry and Applied Biosciences, ETH Zürich, CH-8093 Zurich, Switzerland*

[2]*bp Innovation & Engineering, Applied Sciences bp plc Saltend, Hull, HU12 8DS, United Kingdom*

*Corresponding author: ccoperet@ethz.ch

Abstract

The development of efficient catalysts for the hydrogenation of CO_2 to methanol using "green" H_2 is foreseen to be a key step to close the carbon cycle. In this study, we show that small and narrowly distributed alloyed PtGa nanoparticles supported on silica, prepared via a surface organometallic chemistry (SOMC) approach, display notable activity for the hydrogenation of CO_2 to methanol, reaching 7.2 mol h^{-1} mol_{Pt}^{-1} methanol formation rate with a 54% intrinsic CH_3OH selectivity. This reactivity sharply contrasts with what is expected for Pt, which favors the reverse water gas shift reaction, albeit with a poor activity (2.6 mol h^{-1} mol_{Pt}^{-1}). *In situ* XAS studies indicate that ca. 50% of Ga is reduced to Ga^0 yielding alloyed PtGa nanoparticles, while the remaining 50% persist as isolated Ga^{III} sites. The PtGa catalyst slightly dealloys under CO_2 hydrogenation conditions and displays redox dynamics with PtGa-GaO_x interfaces, responsible for promoting both CO_2 hydrogenation activity and methanol selectivity. Further tailoring the catalyst interface by using a carbon support in place of silica enables to improve the methanol formation rate by a factor of ~5.

Introduction

CO_2 hydrogenation to methanol using "green" H_2 offers an attractive route to mitigate CO_2 emissions and store excess electricity obtained from intermittent renewable energy.[1-3] Extensive efforts have focused on using Cu-based catalysts to convert CO_2 to methanol, since similar catalysts are already commercially implemented in established syngas (CO/H_2)-to-methanol processes.[4-8] However, when CO_2 is used in place of CO as a C_1 feedstock, the Cu-based catalysts suffer from limited activity, methanol selectivity and rapid deactivation as a consequence of the additional water produced.[9] Thus,

alternative catalysts have been investigated to address these challenges, by changing the active metal, e.g. from Cu to Ni or Pd for instance,[10-14] or through including various promoters such as Zn, Ga and In.[15-16]

In that context, recent reports on Ga-promoted systems have enabled to clarify some structure-performance relationships using tailored materials prepared via Surface Organometallic Chemistry (SOMC).[17-18] Detailed operando spectroscopic investigations on a series of well-defined Ga-promoted catalysts (M = Cu, Ni and Pd) supported on silica – $CuGa@SiO_2$,[19] $PdGa@SiO_2$,[20] and $NiGa@SiO_2$[21] – indicate that all systems consist of alloyed MGa nanoparticles under reductive conditions (H_2) and undergo significant de-alloying for M = Cu and Pd under CO_2 hydrogenation conditions, generating an interface between metallic Cu or Pd and GaO_x, which is critical for high methanol selectivity.[19-20] For M = Ni, the system mostly remains alloyed under the same CO_2 hydrogenation conditions, enabling the suppression of the methanation reaction, which is the favored pathway on pure Ni catalyst under the same conditions. Nonetheless, the presence of a small fraction of GaO_x at the interface with the NiGa alloy remains key for methanol selectivity.[21] Overall, both alloying and dealloying, as well as the formation of GaO_x interfaces in dynamic redox processes likely plays an essential role in driving activity and methanol selectivity in these catalytic systems.

Considering the dramatic change in reactivity of Ni and Pd in the presence of Ga and the role of the interface and dynamic redox processes, we became intrigued to understand how Ga and the support would influence the properties of Pt, a metal well-known to catalyze the reverse water gas shift reaction.[22-23] Notably, there is only one example of Pt-catalyzed CO_2 hydrogenation to methanol in batch reactor using 1,4-dioxane as a solvent and Mo as a dopant.[24] In this work, we develop silica-supported PtGa nanoparticles using SOMC and show that this material catalyzes the selective hydrogenation of CO_2 to methanol and that the PtGa-GaO_x interface plays a vital role in stabilizing the key intermediates like formate and methoxy species and promoting methanol formation. We also found that switching the support from silica to carbon enhances the methanol formation rate, further testifying the importance of surface and interfaces in controlling the reactivity of supported metal nanoparticles.

Results and discussion

We started by preparing silica-supported PtGa nanoparticles ($PtGa@SiO_2$) via SOMC. An analogous system was developed earlier in the context of propane dehydrogenation.[25] Here, we selected

Pt allyl-(*N*,*N*'-diisopropyl)acetamidinate, abbreviated as Pt(η^3-allyl)(DIA), a siloxide-free molecular precursor, in order to avoid the formation of additional interfaces from the decomposition of the organic ligands.[26] The synthesis consists of a two-step process, involving grafting of the molecular Pt precursor on silica decorated with isolated Ga^{III} sites ($Ga^{III}@SiO_2$, 1.83 wt% corresponding to ca. 0.8 Ga^{III} nm^{-2}) (Figure S1),[27] followed by a treatment under H_2 to generate supported nanoparticles (Figure 1a). We monitored the preparation process via Fourier Transform Infrared Spectroscopy (FTIR). Upon grafting Pt(η^3-allyl)(DIA) on $Ga^{III}@SiO_2$, the IR band at 3747 cm^{-1} associated with Si-OH almost disappears (Figure 1b), while new bands appear at ca. 3250 cm^{-1} (N-H stretching), 3100-2700 cm^{-1} (C-H stretching), 1700-1600 cm^{-1} (C=N), and 1500-1300 cm^{-1} (C-H bending stretching), consistent with grafting via protonation. After reduction under H_2 at 500 °C, the resulting black solid displays only the characteristic Si-OH group in the IR spectrum with no remaining organic residues. The corresponding monometallic $Pt@SiO_2$ catalyst was prepared analogously using the same precursor, but a silica support, partially dehydroxylated at 700 °C ($SiO_{2\text{-}700}$), in place of $Ga^{III}@SiO_2$ (Figure S2).

Elemental analysis shows that Pt loadings for both materials are similar, in the range of 4.2-4.5 wt%, with Pt/Ga ratio of ca. 1:1 for $PtGa@SiO_2$ (Table S1). High-angle annular darkfield (HAADF) scanning transmission electron microscopy (STEM) images show that the supported nanoparticles on both materials are also similar with a narrow particle size distribution of an average size = ca. 1.9 nm (Figure 1c and Figure S3). Energy dispersive x-ray spectroscopy (EDX) elemental mapping of $PtGa@SiO_2$ shows that the profile of Ga overlaps to a great extent with that of Pt, suggesting the formation of alloyed PtGa nanoparticles after H_2 reduction (Figure S4). This is in line with CO-adsorption IR experiments, which show red-shifted linearly adsorbed CO IR bands by ca. 10 cm^{-1} for $PtGa@SiO_2$ vs. $Pt@SiO_2$, further confirming alloying (Figure 1d).[28-29]

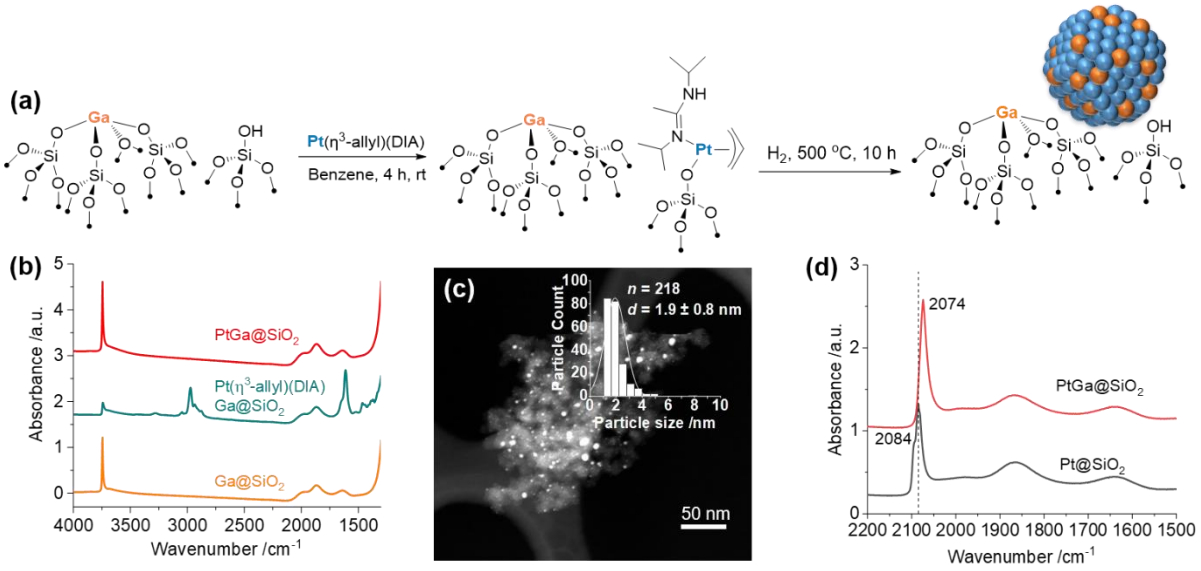

Figure. 1. (a) Schematic procedure for grafting of Pt(η^3-allyl)(DIA) molecular precursor on $Ga^{III}@SiO_2$ followed by reduction under H_2 at 500 °C. (b) FTIR spectra throughout the synthesis of $PtGa@SiO_2$ starting from $Ga^{III}@SiO_2$. (c) STEM image and particle size distribution of $PtGa@SiO_2$. (d) FTIR spectra of CO adsorbed on $Pt@SiO_2$ and $PtGa@SiO_2$ under 5 mbar of CO at room temperature.

The as-prepared bimetallic $PtGa@SiO_2$ and monometallic $Pt@SiO_2$ materials were next evaluated for CO_2 hydrogenation at 230 °C at 25 bar ($H_2/CO_2/Ar$ = 3:1:1). Following a controlled exposure to air, the catalysts were reduced at 300 °C under H_2 prior to CO_2 hydrogenation. The effect of the gas flow rate was also studied to obtain kinetic information related to product formation. Under the aforementioned reaction conditions, $PtGa@SiO_2$ shows a total CO_2 hydrogenation activity reaching 13.5 mol_{CO2} h^{-1} mol_{Pt}^{-1}, which is around 5 times higher than for $Pt@SiO_2$ (2.6 mol_{CO2} h^{-1} mol_{Pt}^{-1}), while $Ga^{III}@SiO_2$ is inactive under the same conditions (Figure 2a). More strikingly, the Ga-promoted catalyst displays an unexpectedly high activity towards methanol formation alone (7.2 mol_{CH3OH} h^{-1} mol_{Pt}^{-1}), with a ca. 50% methanol selectivity, which steadily decreases with increasing CO_2 conversion, the other product being mostly CO as well as a small amount of DME, likely produced from the dehydration of CH_3OH on $Ga^{III}@SiO_2$ sites (Figure 2b and Figure S6).[19-20] The $PtGa@SiO_2$ catalyst performance sharply contrasts with what is observed for the monometallic $Pt@SiO_2$ catalyst, which does not show any methanol but produces CO (≈67%) along with methane (≈33%) (Figure S5). Overall, these results show that a synergy between Pt and Ga promotes CO_2 hydrogenation activity and methanol formation.

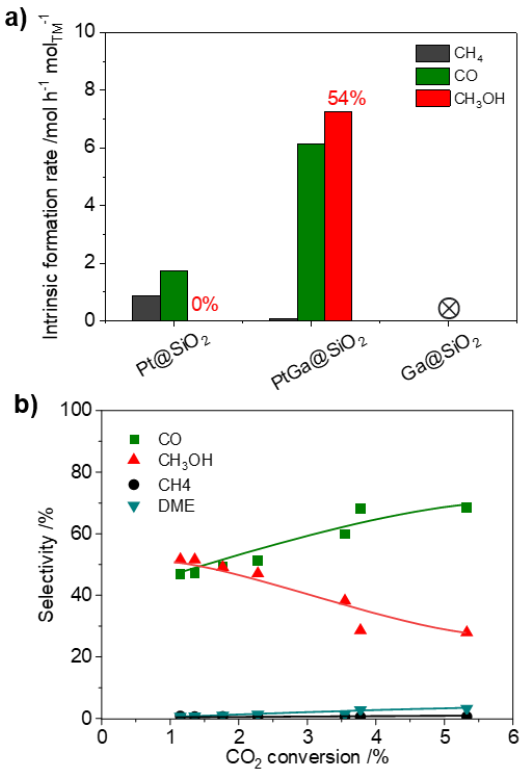

Figure. 2. (a) Intrinsic formation rates over different catalysts. (b) Product selectivities vs CO_2 conversion for PtGa@SiO_2. Reaction conditions: $W_{cat.}$ = 200 mg, F = 6-100 mL/min, T = 230 °C, P = 25 bar.

We next investigated the change of catalyst structure under different conditions (air exposed, reduced under H_2 and post CO_2 hydrogenation) using *in situ* X-ray Absorption Spectroscopy (XAS) experiments. The evolution of the catalyst structure was first analyzed from Pt L_3-edge spectra (Figure 3). The corresponding best-fitting details are presented in Figure S7-S12 and summarized in Table S2. The Pt L_3-edge X-ray adsorption near-edge structure (XANES) spectrum of air-exposed PtGa@SiO_2 is similar to that of Pt foil. The extended X-ray absorption fine structure (EXAFS) spectrum was modeled by using the Pt-Pt scattering path, revealing an average coordination number (CN) of 8.3 for Pt-Pt (Figure S10 and Table S2). After H_2 reduction, Pt L_3-edge XANES indicates a small shift of the edge energy to higher energy along with an increase in white line intensity (Figure 3a). Meanwhile, the intensity of the first peak at ca. 2.1 Å in R space became more intense with respect to the second peak at ca. 2.7 Å (Figure 3b), which can be attributed to the interaction between Ga and Pt, consistent with alloying of the two metals.[30-31] EXAFS fitting reveals the presence of a Pt-Pt scattering path (CN_{Pt-Pt} = 6.1), as well as a low-degeneracy Pt-Ga path (CN_{Pt-Ga} = 2.0). In sharp contrast, the XANES spectra of the monometallic Pt@SiO_2 closely resemble the spectrum of the Pt foil and are all similar under different conditions (Figure 3c and 3d). The fitting results reveal an average CN of Pt-Pt of around 10

(Table S2), which is smaller than for bulk platinum (CN = 12). This is consistent with the presence of small Pt nanoparticles with an expected lower average CN, in line with the observations from STEM measurements.[32] After exposure to CO_2 hydrogenation conditions, the XANES spectra and the CN of Pt-Ga remain quite similar compared to the spectrum of the H_2 reduced catalyst (Figure 3a and 3b), revealing that the PtGa alloy in PtGa@SiO_2 is mostly preserved after reaction, aligning with what is observed for the NiGa system.[21]

We further collected Ga K-edge XANES spectra under identical conditions to gain more insights into the interplay between Pt and Ga in the bimetallic PtGa@SiO_2 system (Figure S13 and S14). The findings show that the Ga K-edge spectrum of the air-exposed PtGa@SiO_2 is similar to the Ga_2O_3 reference. Upon H_2 reduction, the edge energy shifts to lower energy along with a significant decrease in white line intensity, indicating a partial reduction of Ga^{III} into Ga^0, which is incorporated into PtGa nanoparticles (*vide supra*). Linear combination fitting (LCF) analysis shows that ca. half of Ga is reduced and incorporated into alloyed PtGa nanoparticles, resulting in an average Pt/Ga^0 ratio of 1.8:1 (Figure S15 and Table S3), while the remaining Ga (50%) is likely in the state of Ga^{III}@SiO_2.

In addition, both Pt L_3-edge and Ga K-edge *in situ* XANES spectra of PtGa@SiO_2 catalysts were recorded under CO_2 hydrogenation conditions at 230 ^{0}C and 20 bars of gas mixture (H_2/CO_2/Ar = 3:1:1), in order to investigate more subtle variations. The spectra before and after 2 h of reaction are shown in Figure S16. Under *in situ* conditions, the edge position at the Ga K-edge slightly shifts to higher energy along with a slight increase in white line intensity, indicating that Ga is slightly oxidized in the course of the reaction to GaO_x species. On the other hand, there are no significant changes in the spectra at the Pt L_3-edge, indicating that the Pt within the PtGa nanoparticles remains metallic. The combined information indicates that the alloyed PtGa nanoparticles slightly de-alloy under CO_2 hydrogenation conditions to form a PtGa-GaO_x interface. This is consistent with previous reports on Ga-promoted catalysts such as for silica supported CuGa, PdGa and NiGa, where redox dynamics involving *M(M*Ga*)*-GaO_x interfaces play a pivotal role in promoting activity and methanol formation.[19-21] We thus propose that the redox dynamic at the PtGa-GaO_x interface likely lies at the origin of the promotional effect of Ga in CO_2 hydrogenation towards methanol also in the case of PtGa.

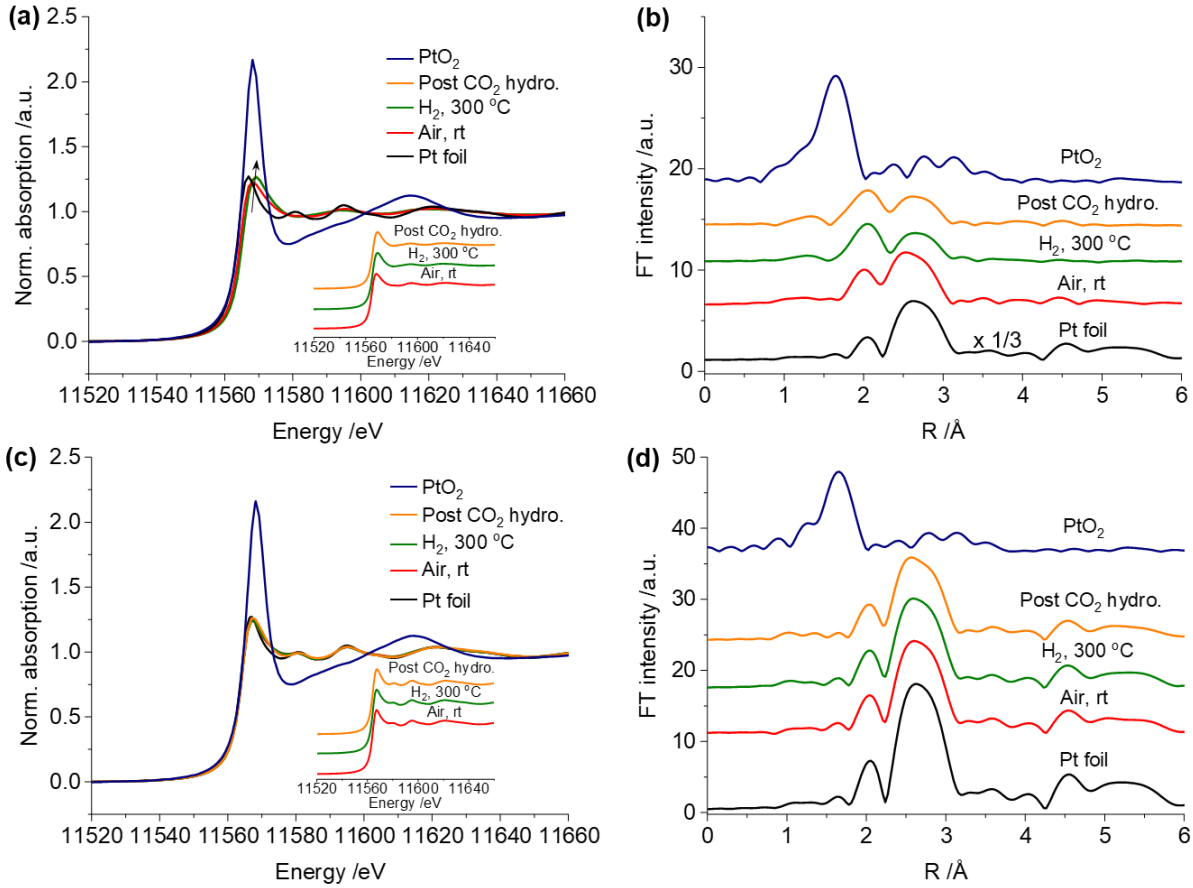

Fig. 3. XANES spectra and corresponding k^3-weighted Fourier transforms of EXAFS spectra at Pt L_3-edge under different conditions (air exposed, H_2 reduced and post CO_2 hydrogenation): (a) and (b) for $PtGa@SiO_2$, (c) and (d) for $Pt@SiO_2$.

Furthermore, *in situ* DRIFTS were performed to observe possible key intermediates over $PtGa@SiO_2$ and $Pt@SiO_2$ during CO_2 hydrogenation at 20 bar. Upon switching to $H_2/CO_2/Ar$ (1:3:1) gas mixture, two CO IR bands appear over $PtGa@SiO_2$ catalyst at ca. 2074 cm^{-1} and 2047 cm^{-1}, and their intensity gradually increases with time on stream (Figure S17). These two bands indicate the presence of two types of Pt sites, likely associated with adsorbed CO* on PtGa and PtGa-GaO_x interfaces, in line with the *in situ* XAS data. After ca. 4 min, new bands appear, whose intensitiy gradually increases with time on stream: the two bands at 2940 cm^{-1} and 2840 cm^{-1} correspond to formate, while these at 2956 cm^{-1} and 2856 cm^{-1} are associated with methoxy species.[33-34] In addition, gaseous CO (2170 cm^{-1}) starts to emerge at ca. 9 min. Note that, in sharp contrast, only adsorbed CO* and gaseous CO are observed over $Pt@SiO_2$. Considering the aforementionned *in situ* XAS results and the literature precedents on Cu-, Ni-, and Pd-based CO_2 hydrogenation catalysts, these findings point to the role of the PtGa-GaO_x interface in stabilizing formate and methoxy intermediates, and promoting

methanol formation under CO_2 hydrogenation.[19-21]

We next decided to examine the influence of the support on the catalytic performance of the PtGa system. Considering that carbon is a more neutral support and less prompt to interfere with the dynamic at the PtGa-GaO_x interface than silica, we thus prepared carbon-supported PtGa nanoparticles (PtGa@C) via SOMC.[35] For this, a mesoporous carbon was first treated in refluxing nitric acid to introduce oxygen functional groups (R-OH),[36] followed by sequential grafting of two siloxide-free precursors $Ga(Mesityl)_3$ and Pt (η^3-allyl)(DIA) to avoid the introduction of an additional oxide interface (Figure S18). Finally, treatment under H_2 resulted in the formation of narrowly distributed PtGa nanoparticles supported on carbon with an average size of 1.4 nm (Figure S23) and a Pt/Ga^0 ratio of ca. 0.9:1 based on elemental analysis and EDX mapping, which is higher than observed for PtGa@SiO_2 (Figure S26 and Table S4). While the average nanoparticle size in PtGa@SiO_2 and PtGa@C are similar, the Pt/Ga^0 ratios within the nanoparticles are different. We thus also prepared PtGa@SiO_2 catalysts with varying Pt/Ga^0 ratios, in order to enable a closer comparison (Figure S19-S27). The materials were denoted PtGa@SiO_2(x:1), where the x:1 represent the nominal ratio of Pt/Ga. LCF analysis indicates that the Pt/Ga^0 ratio within the alloyed PtGa nanoparticles in PtGa@SiO_2(0.5:1) are close to the Pt/Ga ratio of PtGa@C, while still displaying a similar average nanoparticle size of 1.7 nm. (Figure S28 and Table S4).

The as-prepared catalysts were then evaluated in CO_2 hydrogenation (Figure S29-S32 and Table S5). As shown in Figure 4a, PtGa@C displays 21.2 mol_{CH3OH} h^{-1} mol_{Pt}^{-1} intrinsic formation rate for CH_3OH with 56% CH_3OH selectivity, which outperforms most previously reported SOMC based catalysts (Figure S33 and Table S6). In particular, the intrinsic formation rate for CH_3OH on PtGa@C is ca. 5 times higher than that of PtGa@SiO_2 (0.5:1) and the total activity is highest among all of the reported SOMC system so far (Figure S33). In addition, no DME is formed over a wide range of CO_2 conversion on the carbon-supported PtGa@C catalyst (Figure S31), sharply contrasting what is observed for all of the prepared PtGa@SiO_2 catalysts, confirming that DME is formed on Ga^{III}@SiO_2 sites. Notably, the methanol intrinsic formation rate decreases with lower Pt/Ga ratio in PtGa@SiO_2 catalysts, indicating that larger fractions of Ga inhibit the methanol formation (Figure S32). While XAS is not readily possible for PtGa@C catalysts due to the rather low metal loading, we performed CH_3OH temperature programed desorption (CH_3OH-TPD) experiments in order to understand further the role of the presence of Lewis acidic Ga^{III} sites. Overall, no CH_3OH is adsorbed on the carbon support or

PtGa@C, while two distinct desorption peaks at m/z=31 are observed for $Ga^{III}@SiO_2$ as well as the silica-supported PtGa catalyst (Figure S34). The peak at higher temperature can be assigned to the desorption of CH_3OH adsorbed on Lewis acidic $Ga^{III}@SiO_2$ by using SiO_2 as a reference, indicating that CH_3OH can be strongly absorbed on $Ga^{III}@SiO_2$. These observations are consistent with the CO_2 hydrogenation results, where the presence of $Ga^{III}@SiO_2$ was found to suppress the formation rate of CH_3OH by obstructing desorption of CH_3OH (Figure 4b)

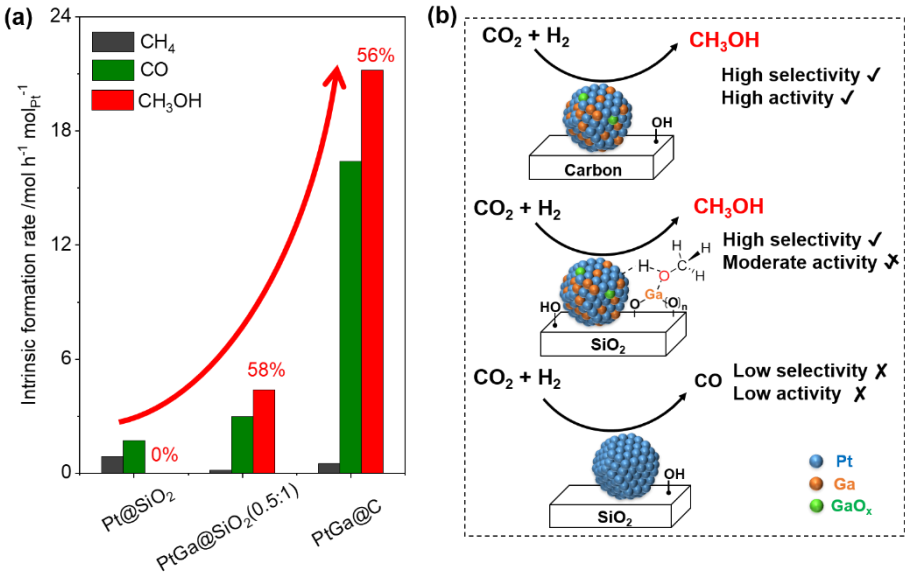

Figure 4. (a) Intrinsic formation rates over different catalysts. Reaction conditions: $W_{cat.}$ = 180-200 mg, F = 6-100 mL/min, T = 230 °C, P = 25 bar. (b) Scheme summarizing the CO_2 hydrogenation outcome over $Pt@SiO_2$, $PtGa@SiO_2$ and PtGa@C catalysts based on the different interfaces.

To summarize, the silica-supported $PtGa@SiO_2$ hydrogenates CO_2 with a 13.2 mol_{CO2} h^{-1} mol_{Pt}^{-1} total activity and a 54% intrinsic methanol selectivity, which greatly contrasts the poor CO_2 hydrogenation performance of monometallic $Pt@SiO_2$, yielding mostly CO and methane under same reaction conditions. Detailed *in situ* XAS analysis indicates, that alloyed PtGa nanoparticles are formed after H_2 reduction, while 50% of Ga remains as Ga^{III}. Under CO_2 hydrogenation conditions, a small fraction of Ga is oxidized to generate PtGa-GaO_x interfaces, which are likely responsible for promoting CO_2 hydrogenation and methanol formation by stabilizing the formate and methoxy species, as evidenced by *in situ* DRIFTS. Altering the interface by replacing silica by a carbon-support further boosts the methanol formation rate by ca. 5, which is due to – at least in part – improving methanol desorption as a result of the absence of Lewis acidic Ga^{III} sites. This study shows that altering the surface and interface of metal nanoparticles like Pt by adding promoters and tuning the support can dramatically

affect the properties of metal sites, thus opening new opportunities for tailoring efficient catalysts, as in the case of CO_2 hydrogenation to CH_3OH, where redox dynamics are thought to play an important role.

Acknowledgements

W.Z. & C.C. thank bp plc for financial support. This publication was created as part of NCCR Catalysis (grant number 180544), a National Center of Competence in Research funded by the Swiss National Science Foundation. Dr. G. J. Sunley is thanked for scientific discussion. The authors acknowledge Dr. W. V. Beek and Dr. D. Stoian at the Swiss Norwegian Beamlines (SNBL, ESRF) for the provision of beamtime and support with *in situ* XAS experiments via proposal A31-1-197. The authors acknowledge N. Zimmerli for the assistance with CH_3OH-TPD and X. Zhou for the assistance with TEM. The authors acknowledge Dr. Y. Wang and C. Wang (Kunming University of Science and Technology) for the assistance with *in situ* DRIFTS. Furthermore, ScopeM is gratefully acknowledged for their support and assistance in this work through project No. 2460 and No. 2568.

Appendix A. Supplementary data

Supplementary data to this article can be found online at xxxx.

References

1. Goeppert, A.; Czaun, M.; Jones, J. P.; Surya Prakash, G. K.; Olah, G. A. Recycling of Carbon Dioxide to Methanol and Derived Products - Closing the Loop. *Chem. Soc. Rev.* **2014,** *43*, 7995-8048.

2. Olah, G. A. Beyond Oil and Gas: The Methanol Economy. *Angew. Chem. Int. Ed.* **2005,** *44*, 2636-2639.

3. Centi, G.; Quadrelli, E. A.; Perathoner, S. Catalysis for CO_2 Conversion: a Key Technology for Rapid Introduction of Renewable Energy in the Value Chain of Chemical Industries. *Energ. Environ. Sci.* **2013,** *6*, 1711-1731.

4. Sahibzada, M.; Metcalfe, I. S.; Chadwick, D. Methanol Synthesis from $CO/CO_2/H_2$ over $Cu/ZnO/Al_2O_3$ at Differential and Finite Conversions. *J. Catal.* **1998,** *174*, 111-118.

5. Behrens, M.; Studt, F.; Kasatkin, I.; Kühl, S.; Hävecker, M.; Abild-Pedersen, F.; Zander, S.; Girgsdies, F.; Kurr, P.; Kniep, B.-L.; Tovar, M.; Fischer, R. W.; Nørskov, J. K.; Schlögl, R. The Active Site of Methanol Synthesis over $Cu/ZnO/Al_2O_3$ Industrial Catalysts. *Science* **2012,** *336*, 893-897.

6. Schumann, J.; Eichelbaum, M.; Lunkenbein, T.; Thomas, N.; Álvarez Galván, M. C.; Schlögl, R.; Behrens, M. Promoting Strong Metal Support Interaction: Doping ZnO for Enhanced Activity of Cu/ZnO:M (M = Al, Ga, Mg) Catalysts. *ACS Catal.* **2015,** *5*, 3260-3270.

7. Shyam Kattel; Pedro J. Ramírez; Jingguang G. Chen; José A. Rodriguez; Liu, P. Active Sites for CO_2 Hydrogenation to Methanol on Cu/ZnO Catalysts. *Science* **2017,** *355*, 1296-1299.

8. Li, M. M.-J.; Zeng, Z.; Liao, F.; Hong, X.; Tsang, S. C. E. Enhanced CO_2 Hydrogenation to Methanol over CuZn Nanoalloy in Ga Modified Cu/ZnO Catalysts. *J. Catal.* **2016,** *343*, 157-167.

9. Álvarez, A.; Bansode, A.; Urakawa, A.; Bavykina, A. V.; Wezendonk, T. A.; Makkee, M.; Gascon, J.; Kapteijn, F. Challenges in the Greener Production of Formates/Formic Acid, Methanol, and DME by Heterogeneously Catalyzed CO_2 Hydrogenation Processes. *Chem. Rev.* **2017,** *117*, 9804-9838.

10. Sharafutdinov, I.; Elkjær, C. F.; Pereira de Carvalho, H. W.; Gardini, D.; Chiarello, G. L.; Damsgaard, C. D.; Wagner, J. B.; Grunwaldt, J.-D.; Dahl, S.; Chorkendorff, I. Intermetallic Compounds of Ni and Ga as Catalysts for the Synthesis of Methanol. *J. Catal.* **2014,** *320*, 77-88.

11. Studt, F.; Sharafutdinov, I.; Abild-Pedersen, F.; Elkjær, C. F.; Hummelshøj, J. S.; Dahl, S.; Chorkendorff, I.; Nørskov, J. K. Discovery of a Ni-Ga Catalyst for Carbon Dioxide Reduction to Methanol. *Nat. Chem.* **2014,** *6*, 320-324.

12. Proaño, L.; Jones, C. W. CO_2 Hydrogenation to Methanol over Ceria-Zirconia NiGa Alloy Catalysts. *Appl. Catal. A-Gen.* **2024,** *669*, 119485.

13. García-Trenco, A.; White, E. R.; Regoutz, A.; Payne, D. J.; Shaffer, M. S. P.; Williams, C. K. Pd_2Ga-Based Colloids as Highly Active Catalysts for the Hydrogenation of CO_2 to Methanol. *ACS Catal.* **2017,** *7*, 1186-1196.

14. Liu, X.; Gu, Q.; Zhang, Y.; Xu, X.; Wang, H.; Sun, Z.; Cao, L.; Sun, Q.; Xu, L.; Wang, L.; Li, S.; Wei, S.; Yang, B.; Lu, J. Atomically Thick Oxide Overcoating Stimulates Low-Temperature Reactive Metal-Support Interactions for Enhanced Catalysis. *J. Am. Chem. Soc.* **2023,** *145*, 6702-6709.

15. Jiang, X.; Nie, X.; Guo, X.; Song, C.; Chen, J. G. Recent Advances in Carbon Dioxide Hydrogenation to Methanol via Heterogeneous Catalysis. *Chem. Rev.* **2020**.

16. Zhong, J.; Yang, X.; Wu, Z.; Liang, B.; Huang, Y.; Zhang, T. State of the Art and Perspectives in Heterogeneous Catalysis of CO_2 Hydrogenation to Methanol. *Chem. Soc. Rev.* **2020,** *49*, 1385-1413.

17. Coperet, C.; Comas-Vives, A.; Conley, M. P.; Estes, D. P.; Fedorov, A.; Mougel, V.; Nagae, H.; Nunez-Zarur,

F.; Zhizhko, P. A. Surface Organometallic and Coordination Chemistry toward Single-Site Heterogeneous Catalysts: Strategies, Methods, Structures, and Activities. *Chem. Rev.* **2016,** *116*, 323-421.

18. Docherty, S. R.; Coperet, C. Deciphering Metal-Oxide and Metal-Metal Interplay via Surface Organometallic Chemistry: A Case Study with CO_2 Hydrogenation to Methanol. *J. Am. Chem. Soc.* **2021,** *143*, 6767-6780.

19. Lam, E.; Noh, G.; Chan, K. W.; Larmier, K.; Lebedev, D.; Searles, K.; Wolf, P.; Safonova, O. V.; Coperet, C. Enhanced CH_3OH Selectivity in CO_2 Hydrogenation Using Cu-based Catalysts Generated via SOMC from Ga(III) Single-sites. *Chem. Sci.* **2020,** *11*, 7593-7598.

20. Docherty, S. R.; Phongprueksathat, N.; Lam, E.; Noh, G.; Safonova, O. V.; Urakawa, A.; Coperet, C. Silica-Supported PdGa Nanoparticles: Metal Synergy for Highly Active and Selective CO_2-to-CH_3OH Hydrogenation. *JACS Au* **2021,** *1*, 450-458.

21. Zimmerlia N. K.; Rochlitz L.; Checchiac S.; Müller C. R.; Copéret C.; Abdala, P. M. Structure and Role of a Ga-Promoter in Ni-Based Catalysts for the Selective Hydrogenation of CO_2 to Methanol. *JACS Au* **2024,** *4*, 237-252.

22. Su, X.; Yang, X.; Zhao, B.; Huang, Y. Designing of Highly Selective and High-temperature Endurable RWGS Heterogeneous Catalysts: Recent Advances and the Future Directions. *J. Energy Chem.* **2017,** *26*, 854-867.

23. Zhu, M.; Ge, Q.; Zhu, X. Catalytic Reduction of CO_2 to CO via Reverse Water Gas Shift Reaction: Recent Advances in the Design of Active and Selective Supported Metal Catalysts. *Trans. Tianjin Univ.* **2020,** *26*, 172-187.

24. Toyao T.; Kayamori S.; Maeno Z.; Siddiki S. M. A. H.; Shimizu K. Heterogeneous Pt and MoO_x Co-loaded TiO_2 Catalysts for Low-Temperature CO_2 Hydrogenation to Form CH_3OH. *ACS Catal.* **2019,** *9*, 8187–8196.

25. Searles, K.; Chan, K. W.; Mendes Burak, J. A.; Zemlyanov, D.; Safonova, O.; Coperet, C. Highly Productive Propane Dehydrogenation Catalyst Using Silica-Supported Ga-Pt Nanoparticles Generated from Single-Sites. *J. Am. Chem. Soc.* **2018,** *140*, 11674-11679.

26. Ehinger, C.; Zhou, X.; Candrian, M.; Docherty, S. R.; Pollitt, S.; Coperet, C. Group 10 Metal Allyl Amidinates: A Family of Readily Accessible and Stable Molecular Precursors to Generate Supported Nanoparticles. *JACS Au* **2023,** *3*, 2314-2322.

27. Searles, K.; Siddiqi, G.; Safonova, O. V.; Copéret, C. Silica-supported Isolated Gallium Sites as Highly Active, Selective and Stable Propane Dehydrogenation Catalysts. *Chem. Sci.* **2017,** *8*, 2661-2666.

28. Lundwall, M. J.; McClure, S. M.; Goodman, D. W. Probing Terrace and Step Sites on Pt Nanoparticles Using CO and Ethylene. *J. Phys. Chem. C* **2010,** *114*, 7904–7912.

29. Kale, M. J.; Christopher, P. Utilizing Quantitative in Situ FTIR Spectroscopy To Identify Well-Coordinated Pt Atoms as the Active Site for CO Oxidation on Al_2O_3-Supported Pt Catalysts. *ACS Catal.* **2016,** *6*, 5599-5609.

30. Filez, M.; Redekop, E. A.; Poelman, H.; Galvita, V. V.; Ramachandran, R. K.; Dendooven, J.; Detavernier, C.; Marin, G. B. Unravelling the Formation of Pt–Ga Alloyed Nanoparticles on Calcined Ga-Modified Hydrotalcites by in Situ XAS. *Chem. Mater.* **2014,** *26*, 5936-5949.

31. Filez, M.; Redekop, E. A.; Galvita, V. V.; Poelman, H.; Meledina, M.; Turner, S.; Van Tendeloo, G.; Bell, A. T.; Marin, G. B. The Role of Hydrogen during Pt-Ga Nanocatalyst Formation. *Phys. Chem. Chem. Phys.* **2016,** *18*, 3234-43.

32. Beale, A. M.; Weckhuysen, B. M. EXAFS as a Tool to Interrogate the Size and Shape of Mono and

Bimetallic Catalyst Nanoparticles. *Phys. Chem. Chem. Phys.* **2010,** *12*, 5562-5574.

33. Tibiletti D.; Goguet A.; Reid D.; Meunier F. C.; Burch R. On the Need to Use Steady-state or Operando Techniques to Investigate Reaction Mechanisms: An in situ DRIFTS and SSITKA-based Study Example. *Catal. Today* **2006**, *113*, 94–101.

34. Collins S. E.; Briand L. E.; Gambaro L. A.; Baltanás M. A.; Bonivardi A. L. Adsorption and Decomposition of Methanol on Gallium Oxide Polymorphs. *J. Phys. Chem. C* **2008**, *112*, 14988–15000.

35. Brack, E.; Plodinec, M.; Willinger, M. G.; Coperet, C. Implications of Ga Promotion and Metal-oxide Interface from Tailored PtGa Propane Dehydrogenation Catalysts Supported on Carbon. *Chem. Sci.* **2023,** *14*, 12739-12746.

36. Mavrokefalos, C. K.; Kaeffer, N.; Liu, H.-J.; Krumeich, F.; Copéret, C. Small and Narrowly Distributed Copper Nanoparticles Supported on Carbon Prepared by Surface Organometallic Chemistry for Selective Hydrogenation and CO_2 Electroconversion Processes. *ChemCatChem* **2020,** *12*, 305-313.